

3D Simulation of Overland Flow

Dayong SHEN, Kaoru TAKARA and Yasuto TACHIKAWA

Synopsis

In this research, overland flow is simulated based on GIS Flow Element (FE), which is represented by a fine cylinder. The height of the cylinder is in direct proportion to the velocity of overland flow; the inclination of the cylinder represents the direction of the movement; the diameter of the cylinder is in direct proportion to the depth of overland flow; and the depth of cylinder color is related to sediment concentration. The deeper the cylinder color is, the greater sediment concentration it represents. Via collecting data from a watershed in China Loess Plateau region and selecting geoscientific models, we simulate the dynamic change of velocity and direction of overland flow in each pixel.

Keywords: overland flow, GIS Flow Element, velocity, direction, geoscientific models, pixel

1. Introduction

Overland flow, which is formed by rainfall and forced by gravity, is flowing water along hillslopes. It will be generated when precipitation exceeds the amount of soil infiltration and depression storage. Usually, overland flow is 3D non-uniform, unsteady and progressive. However, to solve practical problems, related research mainly supposes that the flow is 1D steady, non-uniform and progressive to simplify the computation (Yao, 1993). Since 1920's, many researchers have applied theoretical methods or partially theoretical and partially empirical methods to solve the velocity of overland flow. Some are easy to combine with GIS e.g. the methods proposed by Jiang and Song (1988), Lu (1991) and Yao (1993). Algorithms for tracing the direction of overland flow mainly include 8-neighbourhood method (O'Callaghan and Mark, 1984), multiple nearest neighbor nodes method (Freeman, 1991), random-eight node approach (Fairfield and Leymarie, 1991), 360 directions of flow with the vector-grid algorithm (Mitasova and Hofierka, 1993, Mitasova *et al.*, 1995) and others. Among them, 8-neighbourhood method is accepted as a standard algorithm (Mitasova *et al.*,

1996), which assigns the direction of flow same to the direction of steepest downward slope and has been widely used in hydrology for flow direction mapping and to evaluate hydrological attributes (Shrestha *et al.*, 2005). Approaches for the visualization of overland flow mainly include texture mapping (Ziegler *et al.*, 2001), choroplethic mapping (Taddei *et al.*, 2000; Miller *et al.*, 2002; Soulis *et al.*, 2005), arrowhead method (Wu *et al.*, 1999; Endreny and Wood, 2003) and path sampling (Mitas and Mitasova, 1998) and others. Texture mapping can make a realistic scenario, but it can hardly represent dynamic effects; choroplethic mapping and arrowhead method can make a scenario, which concisely reflects geoscientific principles but lacks the stereoscopic effect. Path sampling is a true 3D method, which can represent dynamic effects but cannot intuitively represent velocity difference. This paper aims at 3D simulation of overland flow based on GIS FE, and utilizes data from a rainfall event in a watershed in China Loess Plateau region to simulate overland flow and shows the information of related parameters pixel by pixel during that event.

2. Overland Flow Simulation based on GIS FEs

2.1 GIS FE

Built based on a pixel from remotely sensed imagery and controlled by geoscientific models, a GIS FE is used for simulating parameters such as velocity and direction of the transport of dynamic soft geobjects and taken as a basic simulation unit. A GIS FE has position, velocity and direction, but neglects volume. The appearance of a GIS FE can be rendered as an arbitrary point, line segment, face or volume. But considering that it is built based on a pixel, the perpendicular projection of a GIS FE in the pixel plane should be completely within the pixel. Via adding color or changing shape, a GIS FE will have more geoscientific attributes.

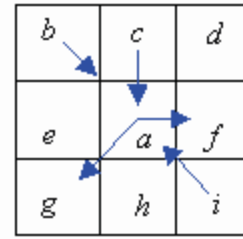


Fig. 1 Schematic map of GIS FEs

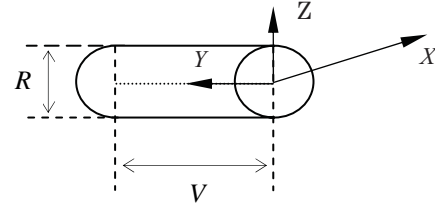


Fig. 2 Geometric structure of a GIS FE

2.2 Simulation of overland flow

Suppose that pixel a is current research objective, b, c, d, e, f, g, h, i are its 8 neighbourhoods (as shown in Figs. 1, 3 and 4). To describe conveniently, an arrow with direction is used to represent the sampled overland flow. Meanwhile, to enhance computation efficiency, 8 directions are used to represent the transport direction of overland flow. Arrows from pixel a to one of its neighbourhoods represent overland flow output of current pixel while arrows from neighbourhoods of a to a represent overland flow input current pixel. Transport route is located in the line segment, which connects the center point of current pixel and the center point of one neighbourhood of a . In this study, overland flow is represented by a streamline structured GIS FE, a fine cylinder (as shown in Fig. 2). The height of the cylinder is in direct proportion to the velocity of overland flow; the inclination of the cylinder represents the direction of the movement; the diameter of the cylinder is in direct proportion to the depth of overland flow; and the depth of cylinder color is related to sediment concentration. The deeper the cylinder color is, the greater sediment concentration it represents. When overland flow runs into river channel, it will not be rendered any more.

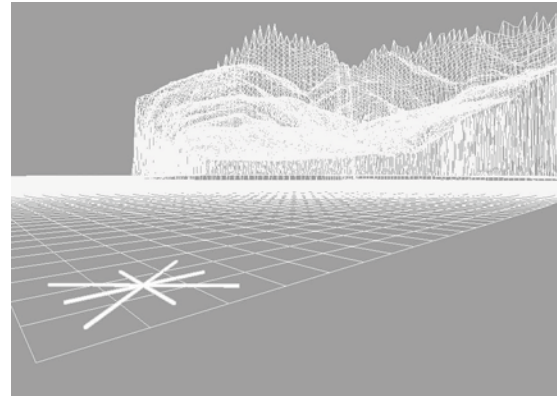


Fig. 3 Schematic map of the transport route for GIS FEs

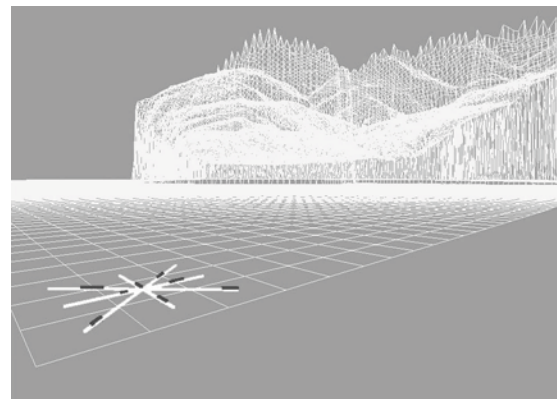


Fig. 4 Schematic map of moving water flow simulation based on GIS FEs

2.3 Geoscientific models

(1) **Flow velocity computation** (as seen in Eq. 1)

$$V = a_0(q/h)^{a_1} S^{a_2} \quad (1)$$

Eq. (1) was built using the method of dimensional analysis and mathematical statistics (Shen *et al.*, 2003), where V is velocity of overland flow (m s^{-1}); q is

discharge per unit width ($\text{m}^3\text{m}^{-1}\text{s}^{-1}$); h is depth of overland flow (m); S is slope angle ($^\circ$); a_0 is geoscientific coefficient and a_1, a_2 are geoscientific indices.

(2) Flow direction tracing

In this study, we simulate overland flow based on pixels from remote imagery. The size for one pixel is $5\text{m} \times 5\text{m}$. DEM of the research area is not complicated. Moreover, we smooth the DEM prior to analysis to reduce the size and number of sinks. Therefore, we use 8-neighbourhood tracing algorithm, which is faster than other flow direction tracing algorithms and suitable for real time rendering of 3D scenarios formed with huge data.

(3) Flow depth computation

Wang et al. (1992) proposed a forecast model of overland flow in hilly and gully regions on China Loess Plateau. Via experiments, the model is proved

practical (as seen in Eq. 2):

$$R = [(P - Z) - FL_u T] P_t C \quad (2)$$

where R is depth of overland flow (mm), P is total precipitation (mm), Z is vegetation interception (mm), F is mean infiltration rate (mm/min), L_u is land use factor, T is rainfall duration (min), P_t is farming measure factor, and C is soil crust factor. Vegetation interception is computed by Hartley method as seen in Eq. 3:

$$Z = Z_{max} C_v \quad (3)$$

where Z_{max} is maximum interception (mm), C_v is vegetation coverage (%). When *S. asperum* was used to do experiments, $Z_{max} = 9.5\text{mm}$ (Wang et al., 1992).

Considering that the leaf surface of *S. asperum* bears burs, which has high water-holding capacity, the value is possibly a little large when it is applied to other vegetations. Additionally, the influence of wind and leaf area index (LAI) has not been contained. Table 1 shows the value of parameters in Eq. (2).

Table 1 Some Factors in the Overland flow Model (Wang et al., 1992)

Parameter	Value	Sample data	Standard Variation	Notes
F_c	0.30			Unit: mm/min
Z_{max}	9.50			Unit: mm
L_u	0.20	50	0.12	Surface soil compaction
	0.23	13	0.16	Shrub and uncultivated slope
	0.33	4	0.14	Forest land
P_t	1.00			
	0.75	20	0.21	Contour farming
	1.25	2		Farming up and down slope
C	1.00			Without crust
	1.50	6	0.23	With crust

(4) Calculation of discharge per unit width (as seen in Eq. 4)

Suppose that water flow denudes and transports surface sediment on hillslope layer by layer, and

rainfall intensity and infiltration rate are stable during Δt , we will get (Lu, 1991):

$$q = x(I - f)\cos S \quad (4)$$

where q is discharge per unit width ($\text{mm}^3 \text{mm}^{-1} \text{s}^{-1}$), x

is the averaged slope length from slope top (mm), S is the averaged slope angle (rad), I is intensity of rainfall (mm min⁻¹), and f is infiltration rate (mm min⁻¹).

(5) Computation of sediment concentration (as seen in Eq. 5)

In China Loess Plateau region, a combination of small mean depth of overland flow with big soil loss (sum of bed load and suspended load) was commonly observed in the field data. This necessitates consideration of the total volume being occupied by the soil sediments, which is normally assumed to make a negligible contribution to the total volume of the water-soil sediment mixture. Then the definition for sediment concentration was derived as follows (Presbitero, 2003):

$$c = \frac{M_S}{V_S + V_W} \quad (5)$$

where c is sediment concentration; M_S is total mass of dry soil sediment, which is computed by erosion model; V_S is total volume occupied by the soil sediment; and V_W is total volume occupied by water.

2.4 Overland flow rendering

(1) Representation and geometry

Table 2 shows 7 parameters of overland flow, which can be well represented by a GIS FE.

(2) Technical route

As shown in Fig. 5, there are mainly 10 steps for simulation of overland flow. We do it based on the platforms of Visual C++ and OpenGL.

(3) Computer rendering

When basic rendering method is applied, we draw each GIS FE as a linear light source with constant color, no luminance or hue difference and no obstacles. Then we accumulate the contribution from each GIS FE, save it into frame buffer and integrate it with normal rendering scenarios as shown in Fig. 6. While advanced rendering method is used, we add light and shadow effect, and delete all GIS FEs in hidden surfaces as shown in Fig. 7.

Table 2 Water flow simulation based on GIS FEs

Parameters	Representation
shape	fine cylinder
colour	light yellow
transparency	semi-transparent
initial position	center point of a pixel
velocity	computed by geoscientific model
direction	8-neighborhoods tracing algorithm
lifetime	Its lifetime will be ended when it moves out of control boundaries.

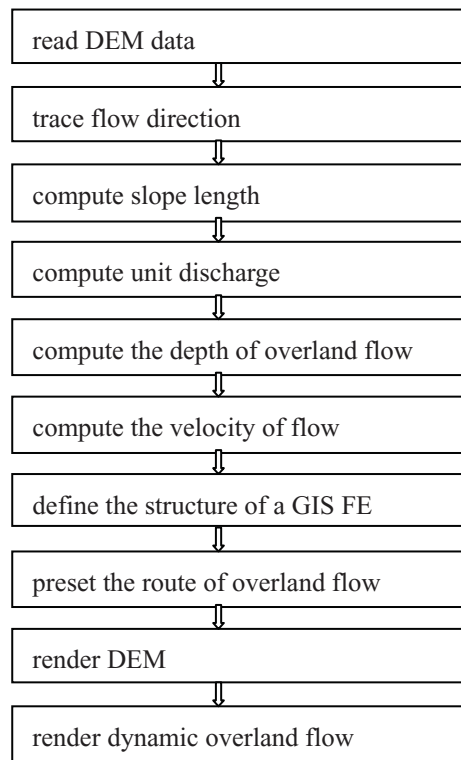


Fig. 5 Flow chart of rendering overland flow

3. Case Study

The experiment plot is Wufendigou small watershed, which is located in Zhunger *Qi*, Inner Mongolia of China. Main data sources: 1:10,000 color infrared aerial photograph, 1:5,000 relief map and measured precipitation. Based on remotely sensed and measured data, we simulate the dynamic change of velocity and direction of overland flow in each pixel as shown in

Figs. 6-7.

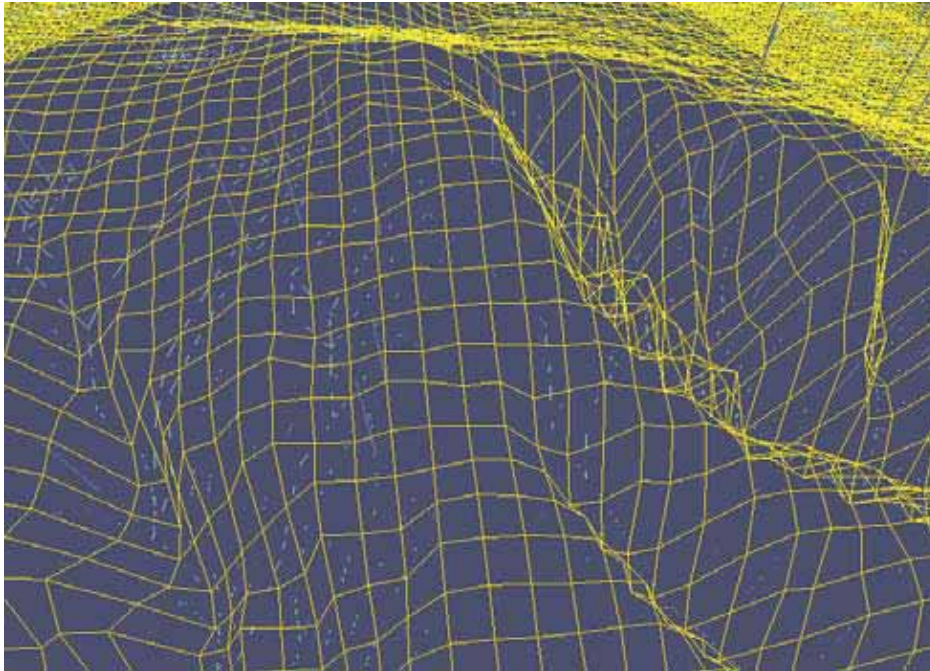


Fig. 6 Grids and GIS FE based overland flow simulation

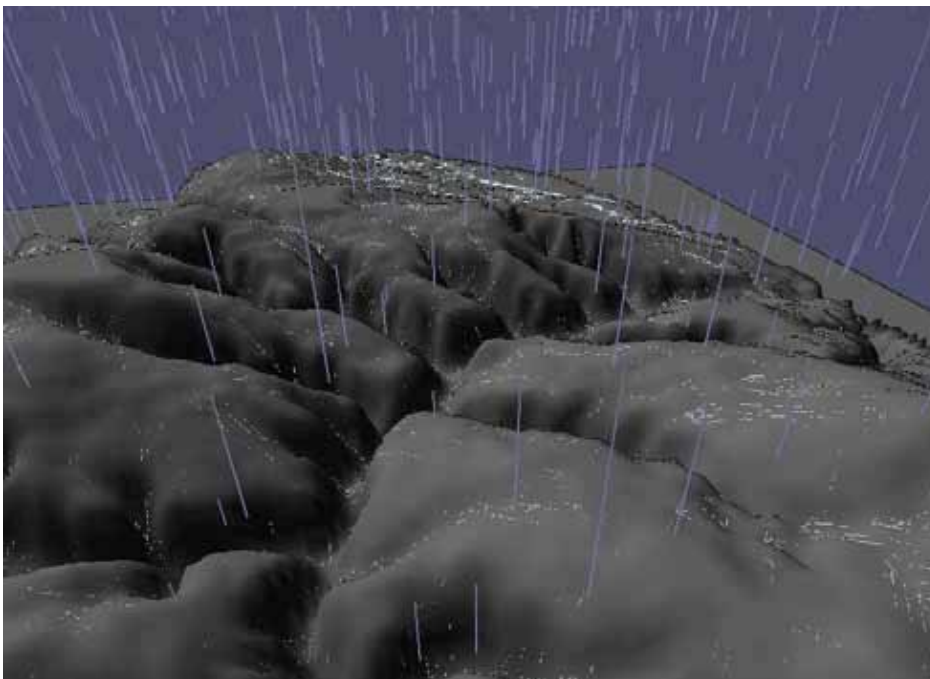


Fig. 7 Overland flow simulation with light and shadow effect

4. Conclusion and Prospects

We apply the approach of GIS FE to represent velocity, direction, depth, transparency and other characteristics of overland flow. Collecting data from China Loess Plateau region, we successfully use computer-rendering skills to generate 3D scenarios,

which can show dynamic overland flow realistically.

Acknowledgment

This research currently is supported by JSPS (Japan Society for the Promotion of Science) Fellowship and the Grant-in-Aid for Scientific Research (No.:

16004360). We are grateful to Takahiro Sayama, Aina Ma, Hui Lin, Zhengping Jin, Hujun Bao and Shanjun Mao for their help and advice.

References

- Endreny, T.A., and E.F. Wood (2003): Maximizing Spatial Congruence of Observed & DEM-Delineated Overland Flow Networks, *International Journal of Geographical Information Sciences*, 17(7), 699-713.
- Fairfield, J. and Leymarie, P. (1991): Drainage networks from grid digital elevation models. *Water Resources Research*, 27, 709-717.
- Freeman, T. G. (1991): Calculating catchment area with divergent flow based on regular grid, *Computers and Geosciences*, 17, 413-422.
- Hofierka, J., Mitasova, H. and Mitas, L. (2002): GRASS and modeling landscape processes using duality between particles and fields. *Proceedings of the Open Source GIS-GRASS Users Conference 2002*. Trento, Italy.
- Jiang, Z. S. and Song, W. J. (1988): Test on flow velocities on hillslopes. *Chinese Academy of Sciences Bulletin of Northwestern Institute of Soil and Water Conservation*, 7, 46-52. (in Chinese)
- Lu, Z. C. (1991): *Watershed Geomorphological Systems*. (Dalian: Dalian Press), pp. 178-180. (in Chinese)
- Miller, S.N., Kepner, W.G. and Ebert, D.W. (2002): GIS-based hydrologic modeling: the Automated Geospatial Watershed Assessment Tool. *Proceedings of the Second Federal Interagency Hydrologic Modeling Conference*, Las Vegas, NV.
- Mitas, L., Mitasova, H. (1998): Distributed soil erosion modeling for effective erosion prevention. *Water Resources Research*, 34, 505-516.
- Mitasova, H., J. Hofierka, M. Zlocha, and R. L. Iverson (1996): Modeling topographic potential for erosion and deposition using GIS, *Int. Journal of Geographical Information Science*, 10(5), 629-641.
- Mitasova, H., and Hofierka, J. (1993): Interpolation by Regularized Spline with Tension: II. Application to terrain modeling and surface geometry analysis. *Mathematical Geology*, 25, 657-669.
- Mitasova, H., Mitas, L., Brown, W.M., Gerdes, D.P., Kosinovsky, I., Baker, T. (1995): Modelling spatially and temporally distributed phenomena: new methods and tools for GRASS GIS. *International Journal of Geographical Information Systems*, 9(4), 433-446.
- O'Callaghan, J. F. and Mark, D. M. (1984): The extraction of drainage networks from digital elevation data. *Comput. Vision Graphics Image Processing*, 28, 328-344.
- Presbitero, A. L. (2003): Soil erosion studies on steep slopes of humid-tropic Philippines. [Doctoral thesis] Griffith University, Queensland, Australia.
- Shen, D. Y., Ma, A. N., Lin, H., Nie, X. H., Mao, S. J., Zhang, B., Shi, J. J. (2003): A new approach for simulating water erosion on hillslopes. *International Journal of Remote Sensing*, 24(14), 2819-2835.
- Shrestha, R., Tachikawa, Y. and Takara, K. (2005): DEM based multi-directional flow path mapping using the raft method. *Proceedings of the International Conference on Monitoring, Prediction and Mitigation of Water-Related Disasters (MPMD-2005)*. 12-15 January 2005, Kyoto University, Kyoto, Japan, 85-90.
- Soulis, E.D., Kouwen, N., Pietroniro, A., Seglenieks, F.R., Snelgrove, K.R., Pellerin, P., Shaw, D.W. and Martz, L.W. (2005): A framework for hydrological modelling in Mags. In: *Prediction in Ungauged Basins: Approaches for Canada's Cold Regions*. Spence, C., J.W. Pomeroy and A. Pietroniro (eds.), Canadian Water Resources Association, 119-138.
- Taddei, U., David, O. and Michl, C. (2000): Application of VisAD in Hydrological Modeling and Simulation. *Computer Graphics (ACM SIGGRAPH)*, 34(1), 48-51.
- Wang, G. P., Jia, Z. J., Cai, Q. G. and Lu, Z. X. (1992): Hillslope runoff prediction model for hilly and gully regions on Loess Plateau in Western Shanxi. *Soil and Water Conservation in China*, 3, 16-20.
- Wu, F. C., Shen, H. W., and Chou, Y. J. (1999): Variation of roughness coefficients for unsubmerged and submerged vegetation." *J.*

Hydraul. Eng., 125 (9), 934–942.

Yao, W. Y. (1993): Research on computation of the velocity of overland flow. Soil and Water Conservation in China, 3, 21-25.

Ziegler, A.D., Giambelluca, T.W., Sutherland, R.A., Vana, T.T. and Nullet, M.A. (2001): Hydrol. Process. 15, 3203–3208.

表面流の3Dシミュレーション

沈大勇・寶馨・立川康人

要旨

本研究は、円筒をGISのフローエレメント（FE）とし、表面流を3次元的に表現する。円筒の高さは表面流の流速に比例し、その角度は表面流の流れの方向に、その直径は表面流の高さに比例する。また、円筒の色は土砂濃度に比例する。提案する手法を中国の黄土高原に適用し、それぞれのピクセルにおける表面流の流速と方向の変化をシミュレートする。

キーワード：表面流，GISフローエレメント，流速，落水方向，地学モデル，ピクセル